Journal of Chromatography A, 1220 (2012) 122–131

Contents lists available at SciVerse ScienceDirect

Journal of Chromatography A

journal homepage: www.elsevier.com/locate/chroma

A two-dimensional, heart-cutting preparative gas chromatograph facilitates highly resolved single-compound isolations with utility towards compound-specific natural abundance radiocarbon (^{14}C) analyses

Gregory Ian Ball[a,*], Li Xu[b], Ann P. McNichol[b], Lihini I. Aluwihare[a]

[a] Scripps Institution of Oceanography, University of California, San Diego, 9500 Gilman Drive #0208, La Jolla, CA 92037, USA
[b] Woods Hole Oceanographic Institution, Woods Hole, MA 02543, USA

ARTICLE INFO

Article history:
Received 28 July 2011
Received in revised form 26 October 2011
Accepted 14 November 2011
Available online 23 November 2011

Keywords:
Preparative capillary gas chromatography (PCGC)
Compound-specific radiocarbon analysis (CSRA)
PCGC optimization
Lignin phenols
Heart-cutting
Deans Switch

ABSTRACT

Motivated by the need to develop clean, high purity preparative enrichments of individual compounds for micro-scale compound-specific natural abundance isotope and radiocarbon (^{14}C) analyses, we describe a new, two-dimensional, heart-cutting, low-bleed, three-oven, *single* GC preparative system, demonstrate its resolving capabilities as applied to a typically complex environmental sample matrix, and investigate the robustness with which it preserves the authigenic $^{13}C/^{12}C$ and $^{14}C/^{12}C$ ratios of individual compounds it targets for preparative enrichment. The system is comprised of a programmable temperature vaporizing (PTV) inlet, a single GC oven, two modular, door-mounted, resistively heated low thermal mass (LTM) columns, a preparative fraction collector (PFC), and a Deans pneumatic switching device which facilitates heart-cutting between the system's 1° and 2° chromatographic dimensions. Further, the system's inlet and trapping parameters are optimized for the efficient preparative enrichment of the methyl ether and ester derivatives of the lignin phenol compound class. The lignin phenols include such compounds as the vanillyl and syringyl aldehydes, ethanones, and acids and are unrivaled biomarkers of terrestrial organic matter, some of which are also important components of fragrances and flavors. Using this suite of compounds, the suitability of this augmented preparative capillary GC (PCGC) system was investigated for micro-scale compound-specific (CS) stable isotope and natural abundance radiocarbon analyses (RA). Analysis of a >300 injection enrichment scheme reveals the instrument to fractionate ^{13}C in predictable ways and to preserve the authigenic $\Delta^{14}C$ of compounds it targets for preparative enrichment to within 6.7 ± 5.0‰, demonstrating the promising new utility of such systems towards micro-scale CSRA investigations for which clean and high resolution separation techniques are prerequisite.

1. Introduction

Radiocarbon is naturally formed in the upper troposphere and lower stratosphere before quickly oxidizing to $^{14}CO_2$ – a molecule of which is present for every trillion (10^{12}) molecules of $^{12}CO_2$. Additionally, above-ground nuclear weapons testing in the 1950s and 1960s doubled the atmospheric ^{14}C inventory. Once oxidized into CO_2, ^{14}C acts as an isotopic tracer and radioactive clock which is entrained into all photosynthetically derived biomolecules before decaying with a 5730-year half-life. Radiocarbon's presence throughout the Earth's active atmospheric, terrestrial, and oceanic components of the Global Carbon Cycle makes compound-specific radiocarbon analysis (CSRA) a powerful tool which enables explorations into the modes and rates of carbon exchange between these reservoirs. It also has the potential to be applied to other purposes, such as towards authenticating the source of chemical additives in consumer products as either natural (^{14}C-containing) or petrochemical derived (^{14}C-dead).

The persistent obstacle to CSRA investigations, however, derives from the challenges inherent to cleanly isolating individual components from the complex environmental matrices in which they are contained [1]. For this reason, preparative enrichments for natural abundance CSRA rely upon efficient, highly resolved, and high purity chemical separations which are explicitly designed to resist contamination by exogenous carbon.

Traditionally, CSRA preparations have been performed using either HPLC [2] or preparative capillary gas chromatography (PCGC) [3]. More recently, a two-step preparative HPLC technique was applied to CSRA investigations of dicarboxylic acids from aerosols [4] and lignin phenols isolated from sediments [5] and plant matter [6]. The greater number of theoretical separation plates in capillary columns, compared to HPLC, has made PCGC more attractive for

* Corresponding author at: Scripps Institution of Oceanography, Marine Chemistry & Geochemistry, University of California, San Diego, 9500 Gilman Drive #0208, La Jolla, CA 92093-0208, USA. Tel.: +1 510 517 6058; fax: +1 858 822 3310.
E-mail address: gball@ucsd.edu (G.I. Ball).

0021-9673/$ – see front matter © 2011 Elsevier B.V. All rights reserved.
doi:10.1016/j.chroma.2011.11.021

natural abundance CSRA analyses because of the clean and highly resolved analytical separations it affords. CSRA investigations relying on PCGC have expanded greatly in the past decade to include the somewhat routine analyses of individual fatty acids, alkanes, and long-chain (C_{37}) alkyl ketones (alkenones) isolated from oceanic [7–11] sediments. One previous exploratory lignin phenol PCGC CSRA study was also reported [12]. PCGC-coupled stable isotope analyses have also been applied to discriminate between natural and fossil sources of polycyclic aromatic hydrocarbons (PAHs) in aerosols [13] and in sediments [14], to identify naturally occurring homologues to polybrominated diphenyl ethers (PBDEs) [15], and to investigate Cl-isotope ratios in polychlorinated dibenzo-p-dioxins (PCDDs) to infer biotic versus abiotic formation mechanisms for these compounds in kaolinite clays [16].

In the case of long chain alkyl PCGC separations, urea adduction is often performed as an essential pre-PCGC clean-up step, partially owing to the limited resolving power of traditional PCGCs, which often necessitates additional upstream cleanup steps. This limited resolving power ultimately derives from traditional PCGCs' single dimensionality, lack of heart-cutting, and their near-exclusive reliance on 'mega-bore' (0.53 mm i.d.) rather than narrower-bore columns, principally because of the greater loading capacities of larger-bore columns which necessitate fewer injections, leading to shortened instrument times. Such larger-bore columns are used despite their significantly reduced resolving power relative to narrower-bore capillary columns whose resolving advantages are described by an inverse-square relationship that relates a halving of column width to a corresponding four-fold *increase* in resolution [17]. As such, the existing separation capabilities of traditional 1D PCGC methods clearly merit improvements which will facilitate high purity, single-compound enrichments from complex samples and which may reduce the need for upstream cleanup steps.

Multi-dimensional GC provides well-known resolving advantages over traditional single-column GC [17]; two columns of varying stationary phase connected in series can resolve components at greater resolutions than are achievable using a single column alone. However, standard 2D methods are fundamentally limited by the diminishing improvements in resolution that are attained with increases in column length. This is because each doubling of column length, while doubling the number of theoretical separation plates (N), only increases peak resolution by a maximum of $\sqrt{\Delta N}$, or 41% [17]. The separation capabilities of such 2D GC methods, however, can be effectively augmented *beyond* this limitation by insertion of a heart-cutting device between the 1° and 2° dimensions. Additionally, as was done in this investigation, resolving power is enhanced by a factor of 4.5 by selection of 0.25 mm analytical columns in lieu of the 0.53 mm mega-bore columns traditionally used in PCGC implementations. While the reduced sample loading capacities of narrower-bore columns necessitate a greater number of repeated injections and longer instrument times, the use of modular low thermal mass (LTM) GC ovens allows for individual GC run times to be shortened.

Such modifications yield a newly implemented, 2D, heart-cutting PCGC approach. In this setup, compounds not targeted for CSRA are discarded while targeted compounds are made to enter, separate, and elute from an additional capillary column interfaced to a preparative fraction collector (PFC). A practical implementation of such a real-time, valve-less switching device was first described by Deans in 1968 [18], adapted to capillary columns, and has more recently been made commercially available by Agilent Technologies as a microfluidic "Deans Switch". Since its inception, the Deans Switch has been implemented in a variety of applications, including analytical process GCs [19] and 2D olfactory detection and MSD GCs [20,21]. It has also been used as a duty-cycling modulator for comprehensive GC × GC [22]. Its suitability for preparative enrichments upstream of compound-specific isotope and radiocarbon analysis, however, has been neither demonstrated nor evaluated.

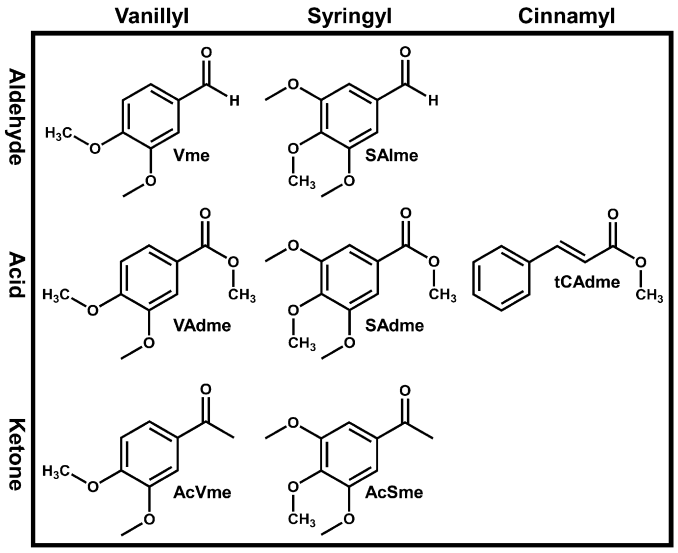

Fig. 1. Structures of the six compounds used to optimize PCGC parameters and evaluate carbon contamination and isotope fractionation imparted by this PCGC system. All compounds except trans-cinnamic acid, methyl ester (tCAdme), are methyl esters and ethers of the lignin vanillyl and syringyl phenolic family: vanillin (V), vanillic acid (VAd), acetovanillone (AcV), syringaldehyde (SAl), syringic acid (SAd), and acetosyringone (AcS). The $-CH_3$ notation and –me suffix for each compound abbreviation show where hydrogens replace $-CH_3$ groups in the corresponding lignin phenols.

Preparative compound enrichments prior to CSRA are essential because accelerator mass spectrometry (AMS) ^{14}C determinations require >30 μg C if the influence of process blank contaminant carbon, usually on the order of 1–4 μg and of inconstant ^{14}C content, is to be adequately constrained [23,24]. Because sample quantities are often limited and because targeted components may only be dilutely present in sample matrices, it is necessary to optimize PCGC instrumental parameters for each targeted compound class to ensure efficient recovery of targeted compounds. In PCGC systems, sample recoveries rarely approach 100%. Analyte losses principally stem from the inlet and the trapping stages of PCGC, but can also arise due to analyte decomposition, irreversible adsorption to system components, and system leaks. The importance of optimizing PCGC collection parameters for different compound classes has been clearly demonstrated for a few model compound types [25], and specifically for PAHs [26], but not yet for the family of phenolic lignin methyl esters and ethers (Fig. 1) described here. Lignin phenols are used to track terrestrial organic matter in the environment [27], and many are also investigated because of their noted contributions to complex flavors and fragrances, of which they are often trace-level, but notable constituents [28,29]. Tracking the radiocarbon signature of these components as they occur in flavors, fragrances, and in the environment offers the potential to provide provenance information of trace additives in complex formulations and to inform the timescales with which terrestrial organic carbon exists in its reduced state (sequestered from the atmosphere) before being re-oxidized to CO_2.

2. Experimental

2.1. Instrumental design

Several commercially available components from Gerstel Inc. and Agilent Technologies were combined to create a two-dimensional, heart-cutting, low-bleed, preparative GC which has

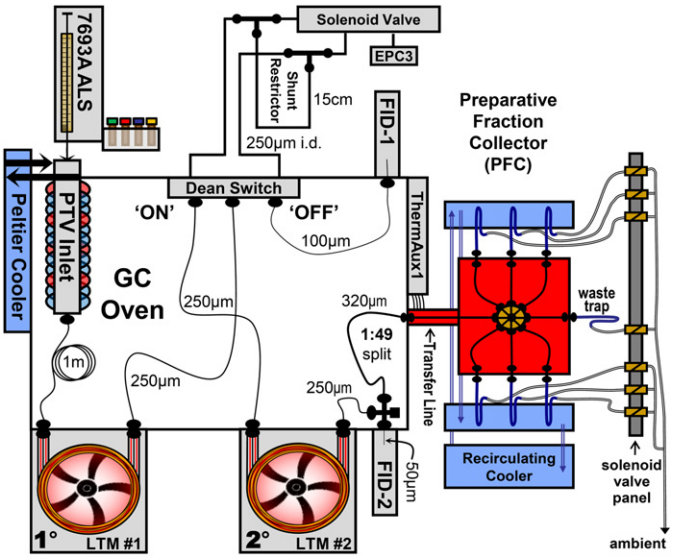

Fig. 2. Schematic of the 2D, heart-cutting PCGC detailed in this paper and whose components are described in Section 2.1. The components shown here are not drawn to scale and their spatial orientation is not representative of the actual configuration. The schematic is instead constructed for ease of visualization.

been schematically outlined in Fig. 2. The setup contains an Agilent 7890A GC, a 7693A Automated Liquid Sampler (ALS), a programmed temperature vaporization (PTV, Gerstel) inlet, two 30 m, 0.25 mm, low thermal mass (LTM, Agilent) capillary columns (1°: Rtx-5MS, 0.50 μm df, 2°: DB-17MS, 0.25 μm df) with mated GC door-mounted transfer line assembles, a zero-dead volume Deans pneumatic microfluidic switching device (Agilent), and a Preparative Fraction Collector (PFC, Gerstel). Inside the Agilent GC oven, 0.25 mm deactivated fused silica tubing (Agilent) routes analytes from the PTV inlet through to the 1° LTM column and into the Deans Switch, which alternately directs flow to the front FID (FID-1) or into the 2° LTM from which it elutes into a four-way splitter. Flow at the four-way splitter is split 1:49 such that ~2% enters the back (FID-2) through a 50 μm i.d. fused silica capillary restrictor while the remaining ~98% continues through 0.32 mm deactivated fused silica tubing which routes analytes through a heated transfer line and into the PFC and its six individual component traps. A 1 m guard column interfaces the PTV with the first column to achieve extended LTM column life. Because the LTM columns are 5″ coils tightly intertwined with temperature sensors and resistively heated coils, they are not readily amenable to periodic column trimming and the use of a guard column is therefore important. The attraction of LTM ovens stems from their modular design, their ability to rapidly heat and cool, and their control from within ChemStation – features that collectively shorten run-times and accelerate preparative GC throughput.

The pneumatic resistance at each Deans switching outlet (labeled ON or OFF in Fig. 2) is equally balanced using deactivated capillary tubing of varying diameters and lengths. Flow direction through the Deans Switch is actuated via a solenoid valve positioned upstream of a shunt restrictor and is controlled within ChemStation as a programmed runtime event. The PFC contains a heated eight-way splitter, which directs eluting analytes into pre-defined component traps by means of a downstream seven-membered solenoid valve array whose valves are programmatically actuated within ChemStation. The traps are U-shaped borosilicate tubes programmed, in this study, to be held at −20 °C (measured to be at −16 °C) using a Haake recirculating cooler. Eluting windows of interest are 'cut' from the 1° column and onto the 30 m 2° column where contaminating interferences present in the 'cut' 1° elution stream are further resolved from those compounds targeted for enrichment. Targeted compounds eluting from the 2° column are then directed into individual component traps where they are frozen and further enriched over repeated injections. In the current study 308 consecutive injections were made. Meanwhile, the contaminating interferences, carryover from the 1° cuts, are directed to a waste trap. Following an enrichment scheme of many repeated injections, the traps can be eluted with high-purity solvents and prepped for CSRA.

2.2. Environmental sample and isotopic (^{13}C, ^{14}C) process standards

Lake Washington Mud (LWM, Seattle, WA) was obtained from Rick Keil (University of Washington, Seattle, WA) and was used to test the resolving capabilities of this system for a widely analyzed and inter-compared environmental reference material [30,31]. To investigate the efficacy of this 2D, heart-cutting PCGC for isotopic and natural abundance ^{14}C investigations, we evaluated a set of eight model compounds (Table 1) whose $^{13}C/^{12}C$ and $^{14}C/^{12}C$ were previously unknown to us. Benzoic acid, methyl ester (bAme, 99%) and benzoic acid, 3,4-dimethoxy-, methyl ester (VAdme, 98%) were obtained from Alfa Aesar. Benzaldehyde, 3,4-dimethoxy (Vme, > 99%), ethanone, 1-(3,4-dimethoxyphenyl)- (AcVme, 98%), and benzaldehyde, 3,4,5-trimethoxy (SAlme) were obtained from Acros Organics. 2-Propenoic acid, 3-phenyl-, methyl ester (tCAdme, 98.7%), benzoic acid, 3,4,5-trimethoxy-, methyl ester (SAdme, 98%), and ethanone, 1-(3,4,5-trimethoxyphenyl)- (AcSme, 98%) were obtained from SigmaAldrich. tCAdme was obtained of certifiably natural origin ($\delta^{13}C = -28.96 \pm 0.04$‰, $^{14}C = 14.91 \pm 0.12$ dpm g C^{-1}). These compounds are shown in Fig. 1 with their relation to their better-known alcoholic, aldehydic, and acidic relatives. All compounds except tCAdme and bAme are methylated ethers and esters of lignin phenolic compounds, which occur naturally in the environment.

Multiple process standards were chosen partly owing to the absence of any *a priori* knowledge of the ^{14}C-content of these process standards, but also because we sought to have a set of process standards with variable $^{14}C/^{12}C$ ratios to enable a more robust evaluation of the $^{14}C/^{12}C$ ratio of any exogenous carbon which might be added throughout a preparative enrichment.

2.3. Evaluation with Lake Washington mud (LWM)

LWM was subjected to CuO oxidation following Goñi and Montgomery's [30] adaption of Hedges and Ertel [31]. Approximately 5 mg organic carbon (100 mg freeze dried and homogenized sediment) was combined with 500 mg CuO, 50 mg $Fe(NH_4)_2(SO_4)_2 \cdot 6H_2O$ and 20 mL 2 N NaOH in a MARS (CEM Corp.) PFA vessel for microwave hydrolysis at 150 °C for 90 min under N_2. The CuO hydrolysate was spiked with ethyl vanillin and trans-cinnamic acid as dual internal recovery standards before being quantitatively decanted into 40 mL EPA vials. The hydrolysate was acidified to pH ~ 2 with 12.1 N trace-metal grade HCl and then extracted 3× with ethyl acetate (Optima). Ethyl acetate extracts were dried over Na_2SO_4 and blown to dryness under ~10 psi N_2 prior to immediate resuspension in 400 μL pyridine. 50 μL of the sample was then diluted 1:1 with pyridine in 400 μL GC vial inserts and derivatized with 100 μL BSTFA + 1% TMCS (Sigma) (60 °C, 10 min) to swap exchangeable protons in the sample mixture with trimethylsilyl (TMS) groups. Injection volume was 5 μL, splitless time was 1 min, vent flow was 100 mL min^{-1}, vent pressure was 1 psi, vent time 0.11 min, and the initial inlet temperature was 100 °C and ramped to 280 °C at 12 °C s^{-1} following a 0.25 min initial time. Compounds were identified based on their retention times (t_R) relative to those of injected standards and were verified on a

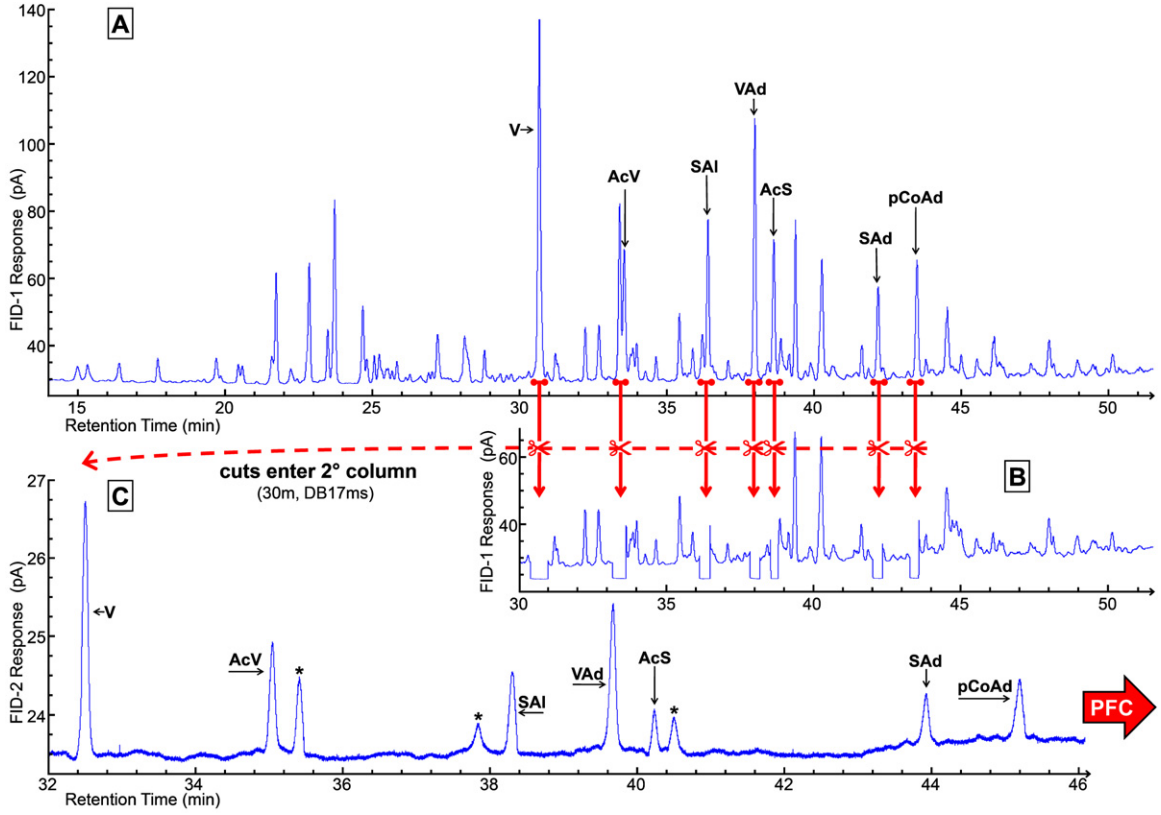

Fig. 3. A complex environmental chromatogram of the alkaline CuO hydrolysate of Lake Washington mud derivatized with trimethylsilyl (TMS) groups. (A) The complex, uncut, original chromatogram visualized by FID-1. (B) Indicated compounds (arrows) are cut to the 2° column in real-time as their excision from the 1° elution stream is observed by FID-1. (C) The cut components enter the 2° column and are further resolved from contaminating interferences (*) before eluting into the PFC as ~2% of the 2° elution stream is diverted to FID-2 for monitoring. Cut intervals were 30.400–31.000, 33.200–33.650, 36.150–36.500, 37.875–38.200, 38.570–38.815, 42.050–42.370, and 43.300–43.600 min. Compound abbreviations follow Fig. 1. pCoAd, *p*-coumaric acid.

GC–MS using an identical column and method. PTV inlet pressure was 38.77 psi, Deans Switch EPC3 pressure was 28.48 psi, carrier gas was He and the system was operated in constant pressure mode. Cut times were determined based on the elution windows of compounds of interest (Fig. 3). GC and (both) LTM ovens were programmed from 100 to 320 °C at 4 °C min^{-1} with a final hold time of 1 min.

2.4. PCGC optimization for lignin ethers and esters

Optimization of PCGC systems is necessary to ensure that targeted compounds are efficiently enriched. Changes in inlet-to-column transfer efficiency were examined by systematically and independently varying PTV inlet parameters while monitoring the FID peak areas resulting from these variations. Changes in PFC trapping efficiencies were also evaluated, but for a more limited set of conditions. All optimizations were performed using a prepared 0.50 mM mixed standard cocktail containing each of the eight compounds listed in Table 1 dissolved in DCM, which was used because of its intermediate polarity and low volatility. Initial LTM oven and solvent venting temperatures were set to 40 °C as no notable improvements in peak shape or analyte transfer efficiency were observed at lower temperatures down to ambient (23 °C).

2.4.1. PTV inlet conditions

Splitless (or purge) times were varied from 0.5 to 3.0 min. FID-1 peak areas were normalized to the area produced using a 60 s splitless time (Fig. 4A). Injection volume was varied systematically from 1 to 5 μL. The resulting changes in peak areas in FID-1 were normalized to μL injected and to the area produced by a 1 μL injection (Fig. 4B). Evaporative concentration of analytes in the PTV inlet is accomplished with solvent venting. The goal of optimizing vent pressure and flow is to selectively evaporate solvent without sweeping targeted analytes out of the split vent. Using a vent time of 0.10 min, vent flow and vent pressure were each varied independently of one another. Vent flow was varied from 30 to 90 mL min^{-1} at a constant vent pressure of 1 psi and the resulting changes in FID areas were normalized to that produced at 30 mL min^{-1} (Fig. 4C). Similarly, vent pressure (the column head pressure) was varied between 1 and 39 psi while vent flow was held constant at 90 mL min^{-1} and the resulting changes in areas were normalized to the area produced at a vent pressure of 1 psi (Fig. 4D). All injection speeds were at 9600 μL min^{-1}.

2.4.2. Trapping conditions

Trapping efficiencies were evaluated using Gerstel Inc's "1 μL" and "100 μL" traps, as well as "100 μL" traps filled with DCM:acetone (1:1, v/v). In these evaluations, the PFC temperature was held at 325 °C and the trap temperatures were maintained at −16 °C. All other variables were held constant. To quantify preparative yields under these conditions, 10–15 repeated injections were made with each trapping configuration. The sample traps were then eluted 3× with DCM:acetone (1:1, v/v) into pre-weighed 4 mL vials. The vials were immediately capped and weighed at 22 °C and then rapidly aliquoted into GC vials, which were quickly capped and immediately analyzed via GC–MS. Quantification of trap contents was achieved using 5-point calibration curves of individual external standards.

Table 1
$\delta^{13}C$ and $\Delta^{14}C$ values of initial and trapped components investigated in this study in addition to trap purities and yields following the 308-injection preparative enrichment.

Samples			Initial			Measured					Differences (‰)		
Short name (trap #)	Cat#, Lot #	%C	NOSAMS ID #	$\delta^{13}C$ (‰)[a]	$\Delta^{14}C$ (‰)[b,c]	NOSAMS ID #	$\delta^{13}C$ (‰)[a]	μg C as CO_2 ($C_{measured}$)	$\Delta^{14}C$ (‰)[c,d]	Yield (%)	Purity (%)	$\Delta\delta^{13}C$[e]	$\Delta\Delta^{14}C$[f]	$\Delta\Delta^{14}C$[g]
												Measured–initial		(Sample–initial)
tCAdme (T1)	12096TH, W269816	74.06	OS-78665	−29.06	79.9 ± 3.6	OS-78867	−28.63	38.6	40.9 ± 3.4	68	100	0.43	−39.0 ± 5.0	−1.1 ± 5.0
Vme (T2)	A0233058, 162610050	65.05	OS-78652	−33.07	−997.5 ± 0.2	OS-78851	−32.33	70.9	−988.9 ± 5.0	60	100	0.74	+8.6 ± 5.0	+3.0 ± 5.0
AcVme (T3)	A01984670, 1688500050	66.65	OS-78653	−33.14	−998.5 ± 0.2	OS-78847	−32.31	72.9	−993.1 ± 5.0	68	100	0.83	+5.4 ± 5.0	−0.1 ± 5.0
VAdme (T4)	10107436, B23568	61.22	OS-78654	−33.55	−993.3 ± 0.3	OS-78848	−32.96	72.3	−996.9 ± 5.0	72	100	0.59	−3.6 ± 5.0	−6.7 ± 5.0
SAlme (T5)	A0174340, 139910250	61.22	OS-78655	−36.10	−998.2 ± 0.2	OS-78833	−36.23	93.1	−990.9 ± 5.0	63	98	−0.13	+7.3 ± 5.0	+3.1 ± 5.0
SAdme (T6)	S29247-308, M8.600–6	58.40	OS-78657	−46.53	−307.8 ± 2.6	OS-78841	−44.87	82.3	−318.1 ± 3.1	67	96	1.66	−10.3 ± 4.0	−0.7 ± 4.0
AcSme (T0, waste)	S29062-149, T6.810–1	62.85	OS-78656	−35.75	−268.6 ± 2.9	OS-78839	−36.00	86.2	−340.4 ± 2.5	69	89[h]	−0.25	−71.8[h] ± 3.8	−63.1[h] ± 3.8

[a] Measured at NOSAMS to 1σ uncertainty of 0.1‰.
[b] Analyzed on the 3 MV Tandetron AMS for samples > 100 μg C. ^{14}C sample splits ranged from 0.43 to 1.0 mg C.
[c] Reported error is the larger of either the internal (Poisson counting statistics) or external AMS error measured.
[d] Analyzed on the NOSAMS 500 kV compact AMS system. ^{14}C sample splits ranged in size from 34 to 90 μg C.
[e] $\Delta\delta^{13}C = \delta^{13}C_{measured} - \delta^{13}C_{initial}$. Uncertainty ($1\sigma$) = ±0.14‰.
[f] $\Delta\Delta^{14}C = \Delta^{14}C_{measured} - \Delta^{14}C_{initial}$. No corrections for blank carbon made.
[g] $\Delta\Delta^{14}C = \Delta^{14}C_{sample} - \Delta^{14}C_{initial}$. $\Delta^{14}C_{sample}$ determined from $C_{measured}$ and $\Delta^{14}C_{measured}$ using measured C_{blank} of 1.73 μg C and a $\Delta^{14}C_{blank}$ of −766.6‰ as described in Section 3.6.
[h] This large discrepancy is expected because all cut and untrapped 2° column eluents enter this trap, four of which were radiocarbon-dead and identified in T0 when it was assayed for purity via GC-FID.

Fig. 4. Optimization of PCGC inlet conditions to promote the efficient transfer of components into the capillary column. Methyl esters and ethers of lignin phenols are identified in Table 1. Analyte-to-column transfer efficiency is monitored by recording FID-1 peak areas as inlet conditions are independently varied. Response areas for four optimized parameters are shown normalized to 60 s for splitless time (A), to 0.5 nmol injected for injection volume (B), to 30 mL min^{-1} for vent flow at 1 psi (C), and to 1 psi for vent pressure at 90 mL min^{-1} (D). Benzoic acid, methyl ester (bAme) was included in the standard cocktail to monitor the response of a compound with physicochemical properties different to those for which the inlet was optimized so that the effect of varying inlet parameter could be monitored more informatively. Error bars are ±1σ.

2.5. Acquisition parameters for CSRA enrichments

The eight compounds in Table 1 were dissolved in DCM and combined into a 0.50 mM mixed standard cocktail, which was used as the starting material for preparative enrichment. Optimized inlet parameters were used. 5 μL of standard cocktail was injected at 9600 μL min^{-1} into a baffled deactivated glass liner packed with deactivated glass wool (Gerstel). The PTV was programmed from 40 °C, with an initial time of 0.20 min, to 275 °C at 12 °C s^{-1} with a final hold time of 5 min. Vent flow was set to 90 mL min^{-1} for 0.10 min at a vent pressure of 1 psi. Splitless time was 2 min. The GC oven temperature was programmed from 300 °C (20 min hold) to 310 °C (3 min hold) at 21 °C min^{-1}. The LTM ovens were programmed with identical temperature programs: 40 °C (2 min hold) to 210 °C (1 min hold) at 40 °C min^{-1}, to 230 °C (1 min hold) at 2 °C min^{-1}, to 310 °C (1.05 min hold) at 20 °C min^{-1}. Inlet pressure was 38.77 psi, Deans Switch EPC3 pressure was 28.48 psi, carrier gas was He and the system was operated in constant pressure mode. Cut and trap times were carefully set based on each compound's 1° and 2° dimension elution times as detailed in Fig. 5. Retention times and areas (via FID-2) were monitored continuously (Fig. 6) to ensure consistency and appropriateness of cut and trap times. Throughout a week-long, 308-injection preparative run, no adjustments to either cut or trap times were needed.

2.6. Quantification of trap contents and purities

Traps were eluted 5× with DCM:acetone (1:1, v/v) (GC Resolv, Fisher) into pre-combusted (450 °C, 6 h), pre-weighed 4 mL vials. Aliquots (10–20 μL) were removed, diluted 20×, and quantified using an Agilent 7890A/5975C GC-FID/EI-MSD using the FID

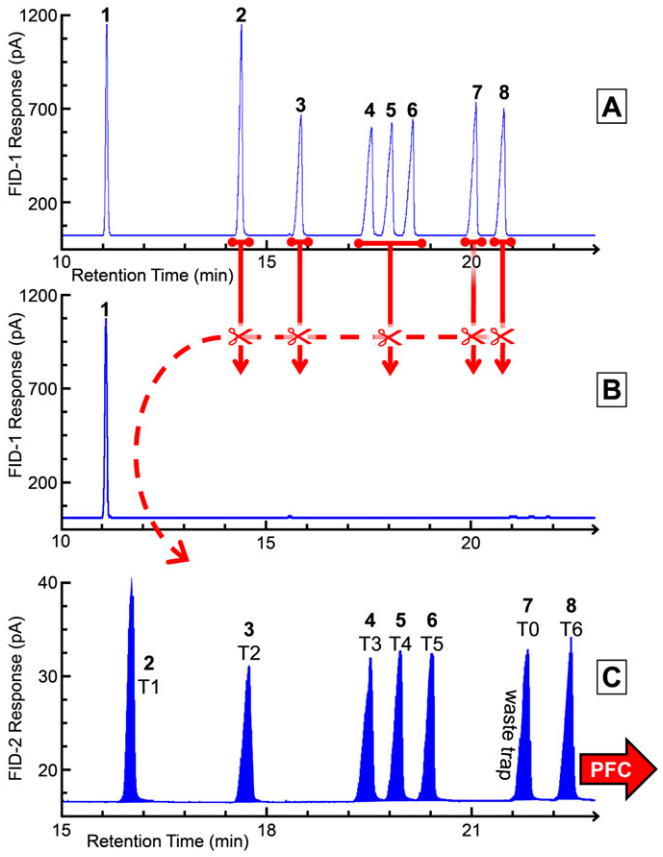

Fig. 5. Chromatograms of the preparative enrichment scheme used for evaluating the suitability of this system for CSRA enrichments. (A) FID-1 visualizes components eluting uncut from the 1° column and (B) when cuts are made. The cuts then enter and elute from the 2° column where ~2% of the elution stream is visualized by FID-2, (C) while the remaining ~98% continues to the PFC where individual compounds are directed into separate component traps prior to CSRA. Cut intervals (arrows) were 14.160–14.900, 15.600–16.100, 17.220–19.000, and 19.770–20.900 min while trapping intervals (shaded peaks) were from 15.82 to 16.20 (tCAdme, T1), 17.45 to 18.05 (Vme, T2), 19.15 to 19.67 (AcVme, T3), 19.67 to 20.12 (VAdme, T4), 20.12 to 20.70 (SAlme, T5) and 22.13 to 22.65 min (T6, SAdme). Numbers atop peaks show corresponding peaks in the three chromatograms. Peak 1 is bAme.

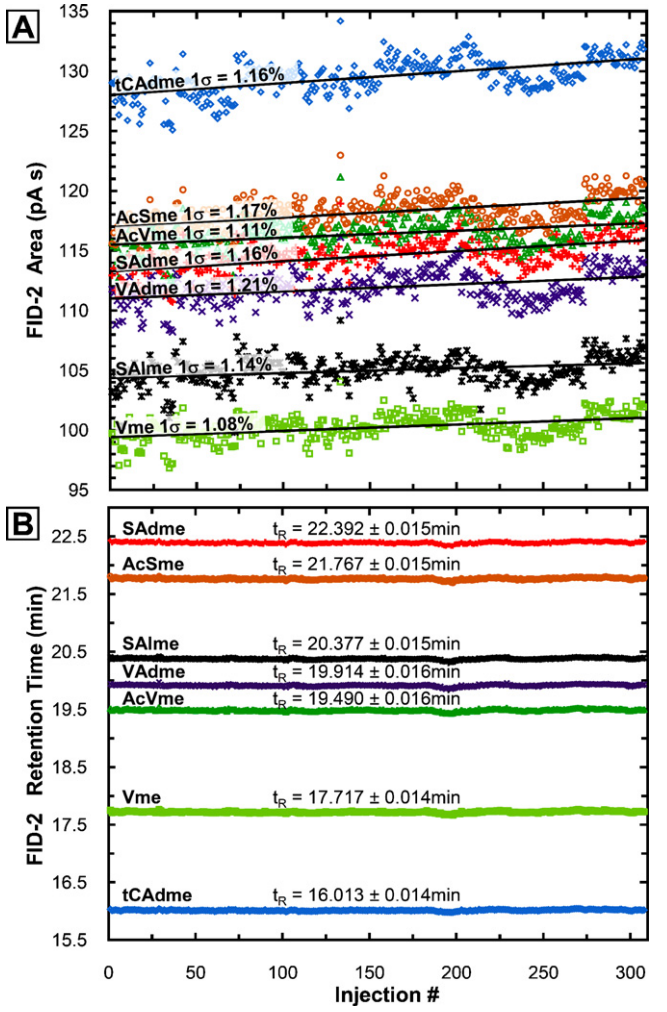

Fig. 6. Stability of the 2D heart-cutting PCGC during the 308-injection preparative enrichment scheme. (A) FID-2 responses for each compound are indicated with their 1σ variability. (B) Stability of retention times (t_R) ± 1σ of cut components eluting from the 2° column into FID-2 and the PFC.

signal and 5-point calibration curves of external standards of the quantified compounds. PCGC recovery yields for each compound were determined following U-tube elution as follows: 100% × (ng of compound trapped)/(ng compound injected). Trap purities were assessed as the ratio of the FID peak area of the targeted compound to that of the total peak area (omitting solvent area) contained within the chromatogram. The remaining volume of eluted samples was then dried gently under N_2.

2.7. ^{13}C and ^{14}C analyses

In preparation for radiocarbon measurements via AMS using the closed tube combustion (CTC) method, samples were resuspended in pentane:dcm (2:1, v/v) and transferred with pre-combusted (450 °C, 6 h) Pasteur pipettes to pre-combusted (850 °C, 6 h) quartz tubes and were again dried under N_2. CuO and silver wire were added to the quartz tube, which was then evacuated and sealed while being immersed in an isopropanol/CO_2(s) slurry (−78 °C). The sealed tube was combusted at 850 °C for 6 h. The evolved CO_2 was cryogenically extracted, quantified, reduced to graphite under H_2 at 630 °C with Fe catalyst, pressed into a graphite AMS target, and analyzed on either a 500 kV or 3 MV Tandetron AMS system following established methods [32] at the National Ocean Sciences AMS (NOSAMS) facility. CO_2 splits were also taken for $^{13}C/^{12}C$ analysis using either a VG PRISM or a VG OPTIMA stable isotope ratio mass spectrometer.

2.8. Reporting of $\delta^{13}C$, $\Delta^{14}C$ data

$^{13}C/^{12}C$ sample ratios are reported in standard $\delta^{13}C$ 'per mil' (‰) notation relative to the Vienna Pee Dee Belemnite (VPDB) standard as follows [33]:

$$\delta^{13}C(‰) = \left(\frac{(^{13}C/^{12}C)_{sample}}{(^{13}C/^{12}C)_{VPDB}} - 1 \right) \times 1000. \quad (1)$$

Measured $^{14}C/^{12}C$ ratios are reported by NOSAMS as fraction modern (Fm) relative to the internationally accepted 'modern' ratio of $(1.176 \pm 0.010) \times 10^{-12}$ which corresponds to 95% of the $^{14}C/^{12}C$ ratio of the 'modern' reference material NBS Oxalic Acid I (in AD 1950) normalized to a $\delta^{13}C_{VPDB}$ of −19‰. Because isotope fractionation may alter the authigenic $^{14}C/^{12}C$ ratios observed in samples, all Fm data are normalized to a $\delta^{13}C$ of −25‰ using the following equation:

$$Fm_{-25‰\,\delta^{13}C} = Fm \left(\frac{1 - 25/1000}{1 + \delta^{13}C/1000} \right)^2, \quad (2)$$

where the magnitude of ^{14}C fractionation is parameterized to be exactly 2× the magnitude of the sample's observed $\delta^{13}C$ fractionation, relative to a $\delta^{13}C$ of −25‰. Radiocarbon results reported here follow the convention of Stuiver and Polach [34] in which sample Fm values are 'age-corrected' back to 1950 and expressed as a per mil deviation from the NBS international standard (in 1950) following:

$$\Delta^{14}C(‰) = (Fm_{-25‰\,\delta^{13}C} \times e^{\lambda(1950-CY)} - 1) \times 1000, \quad (3)$$

where CY is the collection year of the sample (here, 2010 for all samples) and λ is 1/(^{14}C mean life), which corresponds to 1/(8267 years). The reported uncertainties in $\Delta^{14}C$ values are the larger of either the internal machine error (derived from Poisson counting statistics) or the external error (derived from repeated AMS analysis of each graphite target). $\Delta^{14}C$ values > 0‰ reveal the incorporation of ^{14}C derived from above-ground nuclear weapons testing which peaked immediately prior to the ratification of the Nuclear Test Ban Treaty in 1963.

3. Results and discussion

3.1. LWM chromatogram

The chromatogram of the LWM hydrolysate in Fig. 3 demonstrates the augmented resolving capabilities of this high resolution, 2D, heart-cutting PCGC implementation when confronted with a typically complex environmental sample matrix. The LWM 1° chromatogram (visualized uncut with FID-1 in Fig. 3A) exhibits marked co-elution, especially for labeled compounds AcV, SAl, and AcS. However, when these co-eluting components are cut to the 2° column they are observed to undergo further separation during which impurities from the 1° column cuts separate from the components targeted for isolation (seen in Fig. 3C with FID-2). Meanwhile, the *residual* chromatograph containing uncut components is visualized by FID-1 (Fig. 3B), whose monitoring over repeated injections can be used to monitor t_R variability and the appropriateness of programmed cut times. As in other implementations of heart-cutting systems, the performance of the 2° column benefits greatly because it only needs to accommodate cuts from the 1° column, instead of the burden of the entire injected sample (and solvent) handled by the 1° column. In this example, LTM columns were programmed with identical temperature programs. As a result, the full resolving capabilities of this particular setup are perhaps understated for this particular sample. A likely functional improvement to this system could derive from the insertion of a cryo-trap into which 1° column cuts would be directed prior to the onset of 2° column chromatography. Such a modification would likely find utility when trace-level compounds are targeted for CSRA as the cyro-trap facilitates both 'cryo-concentration' (via repeated 1° cuts) and 'cryo-focusing', which would narrow peak widths, further enhancing the instrument's effective resolving power.

3.2. Optimization of inlet and trapping conditions

Improvements in PCGC recoveries resulted primarily from optimization of PTV inlet conditions and secondarily from optimization of PFC trapping conditions. Other unobserved modes of sample loss include system leaks, analyte decomposition or irreversible adsorption to internal instrument surfaces.

3.2.1. Splitless times

Reasonably, longer splitless times were observed to significantly increase inlet-to-column transfer efficiency for all compounds (Fig. 4A). Small increases in inlet-to-column transfer efficiency were noted for splitless times beyond 2 min for all compounds. However, the deterioration of peak shapes beyond times of 2 min made longer splitless times undesirable. The effect of splitless time on inlet-to-column transfer efficiency derives from the time it takes the analytes to enter the column following sample volatilization after rapid inlet heating (12 °C s^{-1}). During this time, volatilized analytes are continuously being diluted in the inlet by incoming carrier gas, which explains why peak shapes were observed to deteriorate beyond 2 min and why longer splitless times achieve maximal transfer of analytes onto the column.

3.2.2. Injection volume

Variations in injection volume (Fig. 4B) indicated that improved inlet-to-column transfer efficiencies could be obtained with larger injection volumes, even after having normalized to the μL of material injected. This indicated that injection volume does not scale proportionally to the amount of material that ultimately enters the column and emphasizes the importance of optimizing this parameter in addition to other adjustable PTV settings if maximal column transfer efficiencies are to be achieved.

3.2.3. Vent flow and vent pressure

The objective of optimizing vent flow and vent pressure conditions is to selectively evaporate solvent while achieving evapo-concentration of targeted analytes inside the glass liner without inadvertently blowing analytes out of the solvent vent. Venting flow, pressure, temperature, and time can all be independently adjusted to tune a PTV system for a particular compound class. Consistent with other PTV inlet assessments [25,26], shorter vent times (0.10 min) were found to provide optimal inlet-to-column transfer efficiencies. Longer venting times adversely affected column transfer efficiencies. Appropriate venting temperatures are informed by the boiling point (b.p.) of the solvent relative to the b.p. of the analytes as well as by the minimum attainable temperature of a particular PTV system (via either Peltier or LN_2 cooling). For the purposes of this work, the inlet temperature was set at 40 °C owing to both the proximity of this temperature to the b.p of the solvent (DCM) and to the speed with which the inlet could be cooled to its initial set-point temperature using the less cumbersome, cryogen-less Peltier PTV cooler. Using these settings, the effect of vent flow and pressure on inlet-to-column transfer efficiency was assessed. Together, the optimization of these two parameters exerted greatest control towards the two-fold goal of selectively evaporating solvent while keeping and concentrating analytes inside the inlet. Independent optimizations of both vent flow and pressure indicated that maximal balancing between selective solvent evaporation and evapo-concentration of analytes in the inlet were obtained at a vent pressure of 1 psi and a vent flow of 90 mL min^{-1}. Vent pressures of ∼1 psi correspond to 'stop-flow' conditions because 1° column flow is effectively stopped when the column head pressure is reduced to near-ambient pressures. Finally, it was observed that a compound with physicochemical attributes different from the lignin-related set analyzed here, bAme, behaved differently with respect to certain PTV parameters, including injection volume (Fig. 4B) and vent pressure (Fig. 4D), emphasizing the importance of performing compound-class specific PTV optimizations to ensure effective and efficient implementations of PCGC.

3.2.4. Trapping conditions

In a study examining PAHs, trapping efficiencies were found to be insensitive either to PFC switch temperature (280 to 340 °C) or to PFC trap temperature (−16 to 30 °C) [26]. It has been reported elsewhere [25], however, that the efficiency with which compounds are isolated using PCGC can be significantly affected by the PFC parameters selected, particularly (1) the temperature of the PFC switch, (2) the temperature of the traps, and (3) the choice of

solvent (or lack thereof) within the component traps. The volatilities of the compounds in the set analyzed here were most similar to two compounds examined in the first study [25] whose recoveries were greatest at sub-ambient trapping temperatures while being largely unaffected by PFC switch temperatures ranging from 280 to 320 °C. Therefore, we chose a sub-ambient trapping temperature of −16 °C and a PFC switch temperature of 325 °C because it was 5 °C above the maximum programmed method temperature and minimized the undesirable possibility of analyte condensation within the PFC switch. With these settings in place, our recoveries ranged from 60 to 72%.

Because the choice of solvent-filled versus empty traps has been previously shown to significantly affect observed PFC recoveries [25] and because we sought to bring our recoveries closer to 100%, we explored whether recoveries for the lignin-related compound set examined here could be improved by use of solvent trapping. We investigated this for traps at −16 °C containing DCM:acetone (1:1, v/v), but no significant increase in PFC recoveries were observed compared to dry traps also maintained at −16 °C. Lastly, Gerstel Inc. offers two PFC trap types (small "1 μL" and large "100 μL") which are shaped and accommodate flow differently. When tested, trapping efficiencies were indistinguishable using either trap type, however the small trap is ultimately more desirable as it requires less solvent to elute, reducing both dry-down times and solvent-derived exogenous carbon contamination.

3.3. t_R Stability and FID reproducibility during a 308-injection enrichment

Because cut and trap times are programmatically defined, small variations in t_R throughout a several-hundred injection run could adversely affect the purities and yields with which targeted compounds are isolated. Fig. 6B shows that despite inclusion of a Deans Switch, an additional 30 m column, and eight additional capillary column connections, this PCGC implementation maintains low t_R variability (max 1σ = 0.016 min), consistent with traditional PCGC setups [3].

The observed variability in FID areas (Fig. 6A) over the seven day, 308-injection scheme ranged from 1.1 to 1.2% ($\pm 1\sigma$). This observed injection-to-injection variability likely derives from the turbulent nature of PTV solvent venting. Such variability is undesirable if precise quantifications are to be achieved, but it poses less of a problem for CSRA enrichments where sample enrichment is the principal objective. However, this variability could underlie observed variability in compound enrichment efficiencies over successive preparative runs. The gradual upward trends in FID areas in Fig. 6A are an understandable consequence of slow solvent evaporation through a repeatedly pierced sample vial septa which was replaced periodically as additional sample aliquots were added.

3.4. Instrumental isotope fractionation

Instrumental methods seeking to discern natural isotope abundances require rigorous investigations into the degree to which they may isotopically fractionate targeted analytes. In PCGC systems, both inverse [35] and normal isotope [36] fractionation effects have been observed for different compounds analyzed in different systems and under different chromatographic conditions. The magnitude of the fractionation has been shown to vary by as much as 5‰ for $\delta^{13}C$ [9], even when care is taken to ensure that whole peaks are collected. Therefore, the degree to which a particular PCGC method fractionates stable isotopes needs to be investigated if its intended enrichments are destined for stable isotope analyses. Additionally, contributions of exogenous "live" or "dead" carbon from a particular PCGC system need to be properly constrained and accounted for to ensure that exogenous carbon does not confound the already-dilute $^{14}C/^{12}C$ (10^{-12}) signal present within an isolated compound.

In all but two instances, trapped compounds were ^{13}C-enriched by an average of 0.85 ± 0.48‰ (1σ) relative to their initial $\delta^{13}C$ value (Table 1). This result could reasonably arise from two sources: (1) excision of ^{13}C-depleted peak tails and (2) preferential evaporative loss of light isotopologues during the drying of samples prior to CTC. Evaporative inlet concentration might be another means of selective evaporation of light isotopologues; however, this effect is likely muted because solvent is only incompletely removed from analytes at this stage.

The first source of isotope fractionation results from the so-called 'inverse isotope effect' [37,38] which predicts ^{13}C-depletion in the tails, and ^{13}C-enrichment in the leads, of capillary column chromatographic peaks. That is, peak tails contain the lighter isotopologues while peak leads contain the heavier isotopologues. Therefore, if peak tails are not wholly cut to the 2° column, or if they are not wholly trapped by the PFC, the contents of the trap will be ^{13}C-enriched. The inverse isotope effect is thought to arise as a consequence of the greater bond strengths present within the heavier isotopologues of a particular compound. The stronger bonds effectively reduce molar volume and molecular surface area, weakening the molecule's interaction with the column's stationary phase. This effect is then amplified as a result of the thousands of repeated gas–liquid thermodynamic equilibrations which occur during capillary column chromatography. This effect is likely accentuated in this particular setup because (1) the narrower-bore columns used here contain a greater N value relative to traditionally used mega-bore columns and (2) peaks are effectively cut twice in this system (once during heart-cutting and again during trapping). The inverse isotope effect was not observed for SAlme, whose $\delta^{13}C_{trap} - \delta^{13}C_{initial}$ was −0.13 ± 0.14‰ (1σ). This likely resulted because the peak tail was better sampled for T5 owing to a more generously defined trap window (Fig. 5). The waste trap (T0) also exhibited slight ^{13}C-depletion (−0.25 ± 0.14‰) relative to the ^{13}C content of the initial AcSme, which was the primary component (89%) collected within this trap. This likely resulted from the collection of ^{13}C-depleted tails of other, incompletely trapped peaks within this trap and whose presence and identity were confirmed when determining the waste trap's purity, which was expectedly low (89%). These observations show that chromatographic conditions and trap times exert observable and significant influence on the observed $\delta^{13}C$ values of trapped compounds and that the 'inverse isotope effect' appears to predominate in the 2D heart-cutting PCGC system described here. Because ^{14}C fractionation is parameterized to be exactly 2× the magnitude of the ^{13}C fractionation, and because $\delta^{13}C$ is always measured in conjunction with ^{14}C determinations, the ^{13}C fractionation observed here should not affect the authigenic $\Delta^{14}C$ value of compounds trapped by this system because all $\Delta^{14}C$ values are normalized to a $\delta^{13}C$ of −25‰ (VPDB).

3.5. Exogenous carbon contamination

$\Delta^{14}C_{measured} - \Delta^{14}C_{initial}$ is negative (Table 1) for those compounds with moderately enriched $\Delta^{14}C$ signatures (>−340‰). This suggests that some amount of exogenous ^{14}C-depleted (<−340‰) carbon is being introduced prior to AMS analysis. Meanwhile, $\Delta^{14}C_{measured} - \Delta^{14}C_{initial}$ is positive (beyond error margins) for three out of four compounds where $\Delta^{14}C_{initial}$ values indicated a lack of measurable ^{14}C (Vme, AcVme, and SAlme), suggesting that blank carbon being introduced is unlikely to be radiocarbon dead and that it has some measurable ^{14}C (i.e., $\Delta^{14}C$ content > −993‰). As described in Section 3.4, isotope fractionation occurring during PCGC or subsequent sample processing is not the source of this

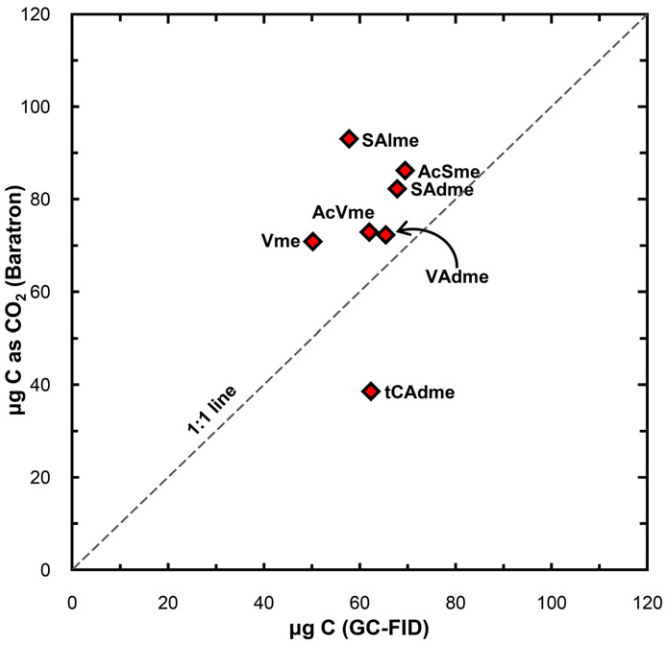

Fig. 7. GC-FID/MS quantification (as μg C) of the trapped component vs. the manometric (Baratron) CO_2 yield of the trap's contents (as μg C) following CTC and cryogenic CO_2 extraction. The data should generally cluster in the vicinity of the 1:1 line, which suggests the absence of either marked sample contamination (most easily detected when samples lie significantly above line) or volatile sample losses (below line) following trap elution and prior to CTC.

difference. To better understand the origins of this blank contaminant carbon contribution, GC-FID quantification of trapped analytes (as μg C) was compared to the manometric CO_2 yield of each trap's contents following CTC and cryogenic CO_2 extraction. In principle, trapped components quantified using each method should agree and plot near the 1:1 line in Fig. 7. In theory, deviations above the 1:1 line are indicative of carbon contamination during PCGC, U-tube elution, sample handling, solvent dry-down and CTC. On the other hand, deviations below the 1:1 line are indicative of sample volatilization losses during sample dry-down stages. Indeed, this was observed with tCAdme, the most volatile compound analyzed, however, contaminant carbon was still likely added, but in an amount less than that lost as a result of tCAdme's volatility. In practice, inaccuracies associated with both the manometric and GC-FID C quantification methods may undermine the quantitative meaningfulness of the *y*-axis of Fig. 7. However, examined together and on a qualitative basis, six of the seven compounds lie above the 1:1 line, providing a secondary indicator beyond $\Delta^{14}C_{measured} - \Delta^{14}C_{initial}$ values that some small measure of carbon contamination is likely present in each of the samples, including tCAdme, which lies below the 1:1 line. Ultimately, if the amount and the $\Delta^{14}C$ content of this exogenous, contaminant carbon are known, the authigenic ^{14}C signal of the compound isolated for CSRA can be extracted.

For this reason, column bleed was assessed as a potential source of ^{14}C-depleted contaminant carbon by heating the 1° and 2° columns to 310 °C and trapping the column bleed eluting at this temperature continuously for 60 min – equivalent to 120 × 0.5 min trapping intervals. The column bleed sample was obtained without repeated solvent injections because solvent is not actively cut to the 2° column during instrument operation and therefore its injection should not affect the 2° column's bleed profile. The trapped column bleed was processed in a manner identical to the sample enrichments, but yielded insufficient carbon (1.73 ± 0.17 μg C) for ^{14}C analysis. The elution of a clean U-tube, following the identical procedure, yielded a statistically indistinguishable amount of carbon (1.63 ± 0.16 μg C) while blank CTC combustions yielded 1.56 ± 0.20 μg C (1σ, n = 3). Together, these data indicate that (1) column bleed was not a major source of contaminant carbon to preparative enrichments and that (2) the observed background contaminant carbon observed here derives from the unavoidable combined processes of U-tube elution, sample handling, sample dry-down, and the combustion blank. PCGC blanks deriving from a combination of these processes have been found to have dead to intermediately dead $\Delta^{14}C$ values generally ranging from −700 to −1000‰ [23,39]. In another PCGC system using a DB-XLB capillary column (30 m, 0.53 mm i.d., 1.5 μm df) [23], column bleed was found to contribute up to 0.6 ± 0.3 μg C min^{-1} of trapping per 50 sample injections, an amount which dropped to 0.1 μg C min^{-1} of trapping per 50 injections when no injection was made and the column saw neither sample nor solvent. In this heart-cutting PCGC the 30 m 2° preparative column coupled to the PFC only comes into contact with the limited amount of sample material heart-cut from the 30 m 1° column (no solvent is cut), significantly reducing the potential contribution of column bleed C into sample traps. Additionally, compared to the thick films of mega bore columns used in traditional PCGC, the choice of thin-film (0.25 μm) and low bleed MS stationary phases in this system further reduces the potential for column bleed.

3.6. Carbon mass balance

If the blank contaminant carbon mass (C_{blank}) and ^{14}C content ($\Delta^{14}C_{blank}$) are known, their contribution to the NOSAMS-measured carbon mass ($C_{measured}$) and ^{14}C content ($\Delta^{14}C_{measured}$) can be used to calculate the unadulterated mass (C_{sample}) and ^{14}C content ($\Delta^{14}C_{sample}$) of the sample using a simple mass balance relationship:

$$\Delta^{14}C_{measured} \cdot C_{measured} = \Delta^{14}C_{sample} \cdot C_{sample} + \Delta^{14}C_{blank} \cdot C_{blank}, \quad (4)$$

where $C_{sample} = C_{measured} - C_{blank}$. If the measured C_{blank} of 1.73 μg C is used in this calculation, then the $\Delta^{14}C_{blank}$ (minimum = −1000‰) can be determined for each trap (T1–T6) using the reasonable assumption that $\Delta^{14}C_{measured}$ should equal $\Delta^{14}C_{initial}$ in the absence of any contaminating blank carbon. 1.73 μg C is chosen because this C_{blank} measurement comes from the column bleed experiment and therefore integrates all contamination introduced from post-PCGC sample handling procedures, including C_{blank} introduced from PCGC column bleed, U-tube elution, sample handling, dry-down, and the combustion blank. When this calculation is performed, the average $\Delta^{14}C$ of the blank carbon contaminating each trap is determined to be −766.7‰, which falls within the −700 to −1000‰ range of PCGC blanks reported elsewhere [23,39].

With values for C_{blank} and $\Delta^{14}C_{blank}$ at hand, $\Delta^{14}C_{sample}$ can be computed from $\Delta^{14}C_{measured}$. When this calculation is performed, the difference ($\Delta\Delta^{14}C$) between the blank-corrected $\Delta^{14}C_{measured}$ (which is $\Delta^{14}C_{sample}$) and $\Delta^{14}C_{initial}$ drops to ≤6.7 ± 5.0‰ for all compounds (Table 1) collected in T1 to T6. Understandably, because the blank's $\Delta^{14}C$ is significantly ^{14}C-depleted, the blank C correction exerts greatest influence on the smallest (μg) and most ^{14}C-enriched compounds. For these reasons, the largest difference between $\Delta^{14}C_{sample}$ and $\Delta^{14}C_{measured}$ is observed for tCAdme.

4. Conclusion

Adaption of 2D heart-cutting techniques to PCGC shows promise towards resolving complex environmental mixtures which normally exhibit recalcitrance towards the baseline-resolved, high-purity separations which are essential for preparative enrichments preceding CSRA. The system is shown to contribute low

amounts of blank carbon to preparative enrichments, preserving the authigenic $\Delta^{14}C$ of sample enrichments to $\leq 6.7 \pm 5.0‰$ between initial and trapped compounds, which is near the limits of AMS precision for small samples. In this implementation of heart-cutting PCGC, an inverse isotope effect is observed, and it is perhaps more pronounced here than in traditional PCGCs because of the narrower columns used (greater N) and because peak tails may be incompletely cut *twice* in this system, once during heart-cutting and again during trapping. For the lignin-related set of compounds analyzed here, no difference was found between the trapping efficiency using solvent-filled traps, the small ("1 μL"), or the large ("100 μL") U-traps used with these PCGC systems. Meanwhile, variability in inlet conditions was found to affect collection efficiency most greatly, and a particular set of conditions providing ideal inlet-to-column transfer efficiency was found, reported, and used for the evaluation of this system for its suitability towards CSRA. A further enhancement to the system would result from insertion of a cryo-trap interfacing the system's 1° and 2° chromatographic dimensions. The absence of detectable column bleed in either blanks or samples collected during >300 repeated injections (over seven days) suggests that heart-cutting PCGC is a lower bleed alternative to traditional PCGC, making it a technique ideally suited for small, ultra micro-scale sample enrichments destined for CSRA.

Acknowledgements

We would like to thank Jeff Lippert and Jack Stuff of Gerstel Technologies for helpful discussions on the effective implementation of Gerstel components in the development of this instrument. This work was aided by the helpful staff at NOSAMS, including Mary Lardie, Al Gagnon, and Mark Roberts, all of whom provided helpful guidance with the generation and interpretation of AMS results. This work was supported by a NOSAMS student internship, the Department of Defense (DoD), National Defense Science and Engineering Graduate (NDSEG) Fellowship (32 CFR 168a), as well as grants from ACS-PRF (45608-AC2) and NSF (MRI OCE-072322, OCE 05–48275) and benefited from the comments of three anonymous reviewers.

References

[1] G. Mollenhauer, J. Rethemeyer, IOP conference ser, Earth Environ. 5 (2009) 1.
[2] R. Gillespie, R.E.M. Hedges, J.O. Wand, J. Archaeol. Sci. 11 (1984) 165.
[3] T.I. Eglinton, L.I. Aluwihare, J.E. Bauer, E.R.M. Druffel, A.P. McNichol, Anal. Chem. 68 (1996) 904.
[4] S.M. Fahrni, M. Ruff, L. Wacker, N. Perron, H.W. Gäggeler, S. Szidat, Radiocarbon 52 (2010) 752.
[5] J. Hou, Y. Huang, C. Brodsky, M.R. Alexandre, A.P. McNichol, J.W. King, F.S. Hu, J. Shen, Anal. Chem. 82 (2010) 7119.
[6] A.E. Ingalls, E.E. Ellis, G.M. Santos, K.E. McDuffee, L. Truxal, R.G. Keil, E.R.M. Druffel, Anal. Chem. 82 (2010) 8931.
[7] M. Uchida, Y. Shibata, K. Kawamura, M. Yoneda, H. Mukai, A. Tanaka, T. Uehiro, M. Morita, Nucl. Instrum. Methods B 172 (2000) 583.
[8] A. Pearson, A.P. McNichol, B.C. Benitez-Nelson, J.M. Hayes, T.I. Eglinton, Geochim. Cosmochim. Acta 65 (2001) 3123.
[9] T.I. Eglinton, B.C. Benitez-Nelson, A. Pearson, A.P. McNichol, J.E. Bauer, E.R.M. Druffel, Science 277 (1997) 796.
[10] E.R.M. Druffel, D. Zhang, X. Xu, L.A. Ziolkowski, J.R. Southon, G.M. Santos, S.E. Trumbore, Radiocarbon 52 (2010) 1215.
[11] M. Uchida, Y. Shibata, K. Ohkushi, M. Yoneda, K. Kawamura, M. Morita, Chem. Geol. 218 (2005) 73.
[12] A.P. McNichol, J.R. Ertel, T.I. Eglinton, Radiocarbon 42 (2000) 219.
[13] H. Kumata, M. Uchida, E. Sakuma, T. Uchida, K. Fujiwara, M. Tsuzuki, M. Yoneda, Y. Shibata, Environ. Sci. Technol. 40 (2006) 3474.
[14] C.M. Reddy, A. Pearson, L. Xu, A.P. McNichol, B.A. Benner, S.A. Wise, G.A. Klouda, L.A. Currie, T.I. Eglinton, Environ. Sci. Technol. 36 (2002) 1774.
[15] E.L. Teuten, L. Xu, C.M. Reddy, Science (New York, N.Y.) 307 (2005) 917.
[16] H. Holmstrand, D. Gadomski, M. Mandalakis, M. Tysklind, R. Irvine, P. Andersson, Ö. Gustafsson, Environ. Sci. Technol. 40 (2006) 3730.
[17] R.L. Grob, E.F. Barry, Modern Practice of Gas Chromatography, 4th ed., John Wiley & Sons, Hoboken, 2004.
[18] D.R. Deans, Chromatographia 1 (1968) 18.
[19] L.F. de Alencastro, D. Grandjean, J. Tarradellas, CHIMIA 57 (2003) 499.
[20] N. Ochiai, K. Sasamoto, J. Chromatogr. A 1218 (2011) 3180.
[21] K. Sasamoto, N. Ochiai, J. Chromatogr. A 1217 (2010) 2903.
[22] J.V. Seeley, N.J. Micyus, S.V. Bandurski, S.K. Seeley, J.D. McCurry, Anal. Chem. 79 (2007) 1840.
[23] L.A. Ziolkowski, E.R.M. Druffel, Anal. Chem. 81 (2009) 10156.
[24] S.R. Shah, A. Pearson, Radiocarbon 49 (2007) 69.
[25] C. Meinert, W. Brack, Chemosphere 78 (2010) 416.
[26] M. Mandalakis, Ö. Gustafsson, J. Chromatogr. A 996 (2003) 163.
[27] R.F. Leo, E.S. Barghoorn, Science 168 (1970) 582.
[28] F.L. Sterckx, J. Missiaen, D. Saison, F.R. Delvaux, Food Chem. 126 (2011) 1679.
[29] M.D. Guillén, M.J. Manzanos, Flavour Frag. J. 20 (2005) 676.
[30] M.A. Goñi, S. Montgomery, Anal. Chem. 72 (2000) 3116.
[31] J.I. Hedges, J.R. Ertel, Anal. Chem. 54 (1982) 174.
[32] A.R. Gagnon, A.P. McNichol, J.C. Donoghue, D.R. Stuart, K. von Reden, Nucl. Instrum. Methods B 172 (2000) 409.
[33] T.B. Coplen, Geochim. Cosmochim. Acta 60 (1996) 3359.
[34] M. Stuiver, H.A. Polach, Radiocarbon 19 (1977) 355.
[35] Z. Zencak, C.M. Reddy, E.L. Teuten, L. Xu, A.P. McNichol, Ö. Gustafsson, Anal. Chem. 79 (2007) 2042.
[36] H. Holmstrand, M. Mandalakis, Z. Zencak, Ö. Gustafsson, P. Andersson, J. Chromatogr. A 1103 (2006) 133.
[37] F. Bruner, G.P. Cartoni, A. Liberti, Anal. Chem. 38 (1966) 298.
[38] M. Matucha, W. Jockisch, P. Verner, G. Anders, J. Chromatogr. 588 (1991) 251.
[39] G.M. Santos, J.R. Southon, N.J. Drenzek, L.A. Ziolkowski, E. Druffel, X. Xu, D. Zhang, S. Trumbore, T.I. Eglinton, K.A. Hughen, Radiocarbon 52 (2010) 1322.